Circulation: Arrhythmia and Electrophysiology

ORIGINAL ARTICLE

Reversible Pulsed Electrical Fields as an In Vivo Tool to Study Cardiac Electrophysiology: The Advent of Pulsed Field Mapping

Jacob S. Koruth, MD; Petr Neuzil, MD, PhD; Iwanari Kawamura, MD; Kenji Kuroki, MD; Jan Petru, MD; Gediminas Rackauskas, MD, PhD; Moritoshi Funasako, MD; Audrius Aidietis, MD, PhD; Vivek Y. Reddy, MD

BACKGROUND: During electrophysiological mapping of tachycardias, putative target sites are often only truly confirmed to be vital after observing the effect of ablation. This lack of mapping specificity potentiates inadvertent ablation of innocent cardiac tissue not relevant to the arrhythmia. But if myocardial excitability could be transiently suppressed at critical regions, their suitability as targets could be conclusively determined before delivering tissue-destructive ablation lesions. We studied whether reversible pulsed electric fields (PF_{REV}) could transiently suppress electrical conduction, thereby providing a means to dissect tachycardia circuits in vivo.

METHODS: PF_{REV} energy was delivered from a 9-mm lattice-tip catheter to the atria of 12 swine and 9 patients, followed by serial electrogram assessments. The effects on electrical conduction were explored in 5 additional animals by applying PF_{REV} to the atrioventricular node: 17 low-dose ($PF_{REV\text{-}LOW}$) and 10 high-dose ($PF_{REV\text{-}HIGH}$) applications. Finally, in 3 patients manifesting spontaneous tachycardias, PF_{REV} was applied at putative critical sites.

RESULTS: In animals, the immediate post-PF_{REV} electrogram amplitudes diminished by 74%, followed by 78% recovery by 5 minutes. Similarly, in patients, a 69.9% amplitude reduction was followed by 84% recovery by 3 minutes. Histology revealed only minimal to no focal, superficial fibrosis. $PF_{REV\text{-}LOW}$ at the atrioventricular node resulted in transient PR prolongation and transient AV block in 59% and 6%, while $PF_{REV\text{-}HIGH}$ caused transient PR prolongation and transient AV block in 30% and 50%, respectively. The 3 tachycardia patients had atypical atrial flutters (n=2) and atrioventricular nodal reentrant tachycardia. PF_{REV} at putative critical sites reproducibly terminated the tachycardias; ablation rendered the tachycardias noninducible and without recurrence during 1-year follow-up.

CONCLUSIONS: Reversible electroporation pulses can be applied to myocardial tissue to transiently block electrical conduction. This technique of pulsed field mapping may represent a novel electrophysiological tool to help identify the critical isthmus of tachycardia circuits.

GRAPHIC ABSTRACT: A graphic abstract is available for this article.

Key Words: catheters ■ electroporation ■ follow-up studies ■ swine ■ transients and migrants

During invasive electrophysiological catheter mapping of organized tachycardias, mapping techniques such as activation and entrainment mapping are typically used to delineate the arrhythmia circuit and identify critical regions to target for catheter ablation.[1] However, these mapping techniques may provide only general localization for ablation targeting. Typically, the criticality of a putative target location can only be definitively

Correspondence to: Vivek Y. Reddy, MD, Helmsley Electrophysiology Center, Icahn School of Medicine at Mount Sinai, Guggenheim Pavillon, Suite 280, 1190 Fifth Ave, New York, NY 10029. Email vivek.reddy@mountsinai.org

Supplemental Material is available at https://www.ahajournals.org/doi/suppl/10.1161/CIRCEP.123.012018.
For Sources of Funding and Disclosures, see page 570.

Circulation: Arrhythmia and Electrophysiology is available at www.ahajournals.org/journal/circep

WHAT IS KNOWN?

- Pulsed field ablation involves the application of high-intensity electrical fields to ablate tissue by a mechanism of irreversible electroporation.
- Low-intensity electrical fields have been used for decades to reversibly electroporate cells, causing transient cellular membrane instability allowing the introduction of biological materials (plasmids, impermeable drugs, etc) without cell destruction.

WHAT THE STUDY ADDS

- When low-intensity pulsed electric fields were applied in vivo to porcine atrial tissue with a lattice-tip catheter, the local electrogram amplitude immediately diminished but gradually recovered over several minutes, thus indicating the reversible effect of these electroporation pulses.
- In other preclinical porcine experiments, the reversible electroporation pulses caused transient PR prolongation and transient AV block in a dose-dependent fashion, thus indicating that these reversible pulses could transiently block electrical conduction.
- In a proof-of-concept series of 2 patients with atypical atrial flutter and 1 with atrioventricular nodal reentrant tachycardia, reversible pulses reproducibly terminated the tachycardias when applied to putative critical sites; pulsed field ablation lesions at the same site resulted in noninducibility.

Nonstandard Abbreviations and Acronyms

AF	atrial fibrillation
AVNRT	atrioventricular nodal tachycardia
LA	left atrium
PFA	pulsed field ablation
PFM	pulsed field mapping
PF_{REV}	reversible pulsed electric field
RA	right atrium
RFA	radiofrequency ablation

known by whether an applied ablation lesion terminates, and renders noninducible, the tachycardia. An unfortunate consequence of this lack of mapping specificity is that ablative energy applications can inadvertently be delivered to innocent cardiac tissue not relevant to the target arrhythmia.

For catheter ablation, recent studies have demonstrated advantages to pulsed field ablation (PFA) over conventional ablation using thermal energy. This nonthermal energy modality uses high-voltage electrical fields for microsecond durations to cause irreversible electroporation, and thus destabilization, of cell membranes, culminating in cell death.[2] Strikingly, preclinical and clinical studies have demonstrated that PFA enjoys a degree of tissue specificity such that the myocardium can be preferentially ablated with minimal to no effect on certain adjacent nonmyocardial tissues such as the esophagus and phrenic nerve.[3–9] These potential safety advantages of PFA have engendered tremendous enthusiasm and prompted clinical trials in treating atrial fibrillation (AF).[10–17]

In addition to irreversible electroporation during PFA, it has also been known for decades that lower intensity pulsed electrical fields can reversibly electroporate cells.[2,18,19] Instead of dielectric breakdown of cell membranes and cell death, attenuated pulses cause transient cell membrane permeability, an effect that has been opportunistically used for introducing various biomaterials (impermeable drugs, genetic materials, etc) into cells.[20,21] By extension, purposeful application of such sublethal electrical pulses to myocardium could result in temporary changes in myocardial electrical properties, without permanently injuring the target myocardium.

We hypothesized that reversible pulsed electric fields (PF_{REV}) would temporarily alter the local myocardial electrical properties and hence electrical conduction, potentiating what we conceptualized as pulsed field mapping (PFM). To assess the feasibility of this concept, we conducted a series of experiments. First, we studied the effects of PF_{REV} delivered in vivo to porcine atrial tissue followed by human atrial tissue. Subsequently, to determine its effect on the conduction system, PF_{REV} were delivered to the porcine atrioventricular node to explore reversible block of atrioventricular node conduction. Finally, to establish the clinical proof of principle of PFM, PF_{REV} applications were delivered to putative critical regions of stable circuits in a small series of patients with spontaneous atrial tachycardias.

METHODS

Overview

All preclinical experiments were approved by the Institutional Animal Care and Use Committee at the Mount Sinai Hospital, New York. A total of 14 Yorkshire swine (50–65 kg) were included in this evaluation. The clinical portion of this report included a total of 12 patients who were a subset of patients enrolled in a first-in-human, prospective, multicenter, single-arm, clinical studies of AF ablation using a focal PFA catheter (URL: https://www.clinicaltrials.gov; unique identifiers: NCT04141007 and NCT04194307).[14] The trial was funded by Affera, Inc (Braintree, MA), the manufacturer of this system. The study was approved by the hospital ethics committees and regulatory agencies and was conducted in accordance with the Declaration of Helsinki. Informed consent was obtained from all subjects. The authors had full access to the primary data, take full responsibility for its accuracy and integrity, performed the analyses and interpretation, made the decision to publish, wrote all drafts, and had final authority over the manuscript content. The data and methods used in the analysis and materials used to conduct the research are not available for access.

Mapping/Ablation Catheter and Electroanatomical Mapping System

The lattice-tip ablation catheter (Sphere-9; Affera, Inc) used in this study has been previously described in detail.[8,14] Briefly, the 8F deflectable catheter uses an expandable, 9-mm-diameter spherical nitinol lattice electrode tip that serves both as a mapping and ablation catheter. The catheter is able to perform either radiofrequency ablation (RFA) or PFA using high-current radiofrequency and PF generators with a saline pump and an electroanatomical mapping system with magnetic localization (Figure S1).[8,14] The lattice tip contains 9 mini-electrodes on the spherical surface and a central indifferent electrode not in tissue contact. The dual-generator design allows facile toggling between delivering radiofrequency or PF energy to the entire spherical lattice tip and utilization of a single electroanatomic map for the procedure.

Bipolar electrograms are configured between each mini-electrode and the center electrode. Each mini-electrode incorporates a temperature sensor for temperature-controlled saline-irrigated RFA from the entire conductive lattice tip. Saline is sprayed from a central irrigation nozzle at 4 or 15 mL/min during mapping or during RFA, respectively. Radiofrequency energy applications were typically of 5-s duration, with a target surface temperature of 73 °C.[8,14]

During PFA, the lattice tip delivered a proprietary biphasic, monopolar PF waveform, consisting of an ungated train of microsecond-scale pulses delivered over 4 s (current output, 21–32 A).[14] For PFM, the PF_{REV} pulse waveform was significantly shorter to a fraction of a second in duration. The current output for the PF_{REV} pulse waveform was 32 A, and the duration settings for the low-dose ($PF_{REV\text{-}LOW}$) and high-dose ($PF_{REV\text{-}HIGH}$) reversible waveforms were <10 ms and >10 ms, respectively. Saline irrigation was set to 4 mL/min throughout mapping and PFA/PF_{REV} delivery. The entire lattice tip delivers PFA/PF_{REV} pulses, but in contrast to RFA, the thermocouples play no energy modulatory feedback role during PFA.

Preclinical Workflow

After an overnight fast, swine were induced with 1.4 mg/kg telazol, 1.1 mg/kg acetylpromazine, and 0.05 mg/kg IM atropine. The animals were ventilated with oxygen and 1.5% to 2.5% isoflurane after intubation. Bilateral femoral venous access was obtained, and following a single transeptal puncture, a deflectable sheath was placed into the left atrium (LA) under fluoroscopic and intracardiac echocardiographic guidance. Intravenous heparin was given for a target activated clotting time of 300 to 350 s. Serial evaluations of PF_{REV} were performed at remote atrial sites in swine that were undergoing serial pulsed field dosing assessments.

Experiment 1 (Atrial Myocardium)

PF_{REV} energy was applied to right atrial (RA) and LA sites in 6 animals under electroanatomical mapping guidance. Following delivery, the catheter tip was held in place without displacement, and bipolar electrograms were continually recorded. For electrogram amplitude analysis, among the 9 simultaneous mini-electrode data, the average of the 2 highest amplitude electrograms was selected and serially measured over time from the point of just pre-PF_{REV} application up to 5 minutes after. Pacing thresholds at 2 ms pulse width were also assessed (pacing delivered from the entire lattice tip) before and after PF_{REV} delivery at select sites.

In 2 of 6 animals, a PF_{REV} application was placed between 2 discrete ablative radiofrequency applications (delivered by the same catheter tip: 5-s RFA lesions under temperature control to a target of 73 °C) to facilitate PF_{REV} site identification at necropsy (Figure 1A). These 2 animals were survived for ≈2 weeks and then underwent high-density mapping (Carto3 V4 System; Biosense Webster, Inc, Irvine, CA) to assess the bipolar voltage at the sites of the contiguous radiofrequency and PF_{REV} applications. After euthanization, the hearts were extracted and stained with triphenyl tetrazolium chloride, following which all sites were closely examined and select tissue specimens sent for histological assessment. After standard formalin fixation, the tissue was processed and stained with hematoxylin and eosin and elastin Masson trichrome.

Experiment 2 (Atrial Myocardium)

PF_{REV} pulses (2–5 per animal) were delivered within the length of the RA and LA appendages in 6 animals. These applications were delivered sequentially without any intervening pause. The animals were humanely euthanized 30 days later, and hearts were extracted and stained with triphenyl tetrazolium chloride followed by careful gross pathological evaluation of both appendages. The RA appendage tissue was selected and submitted for histopathologic analysis. Discrete parallel sections were prepared, processed, and stained with hematoxylin and eosin and Masson trichrome.

Experiment 3 (AV Nodal Tissue)

In 5 additional animals, PF_{REV} pulses were delivered to the AV node–His bundle region identified by high-density electroanatomic mapping (Figure 2A). Applications were delivered using 2 different PF_{REV} pulse formulations: one a low dose ($PF_{REV\text{-}LOW}$) and the other a high dose ($PF_{REV\text{-}HIGH}$). Importantly, the PF_{REV} applications were delivered multiple times at each location (raising the possibility of cumulative effects, as discussed below). Following each application, the catheter tip was maintained in position, and AV conduction was analyzed.

Clinical Populations and Workflow

Patients eligible for the first-in-human clinical trial were adults with symptomatic paroxysmal or persistent AF resistant to at least 1 class I to IV antiarrhythmic medication and were planned for a first-ever ablation procedure, with left ventricular ejection fraction >40% and LA size ≤5.5 cm. Detailed inclusion/exclusion criteria are in the Supplemental Material. During the AF ablation procedures, there were 2 types of PF_{REV} evaluations: cohort number 1 (n=9 patients) was a post- PF_{REV} electrogram amplitude analysis similar to preclinical experiment number 1 (above), and cohort number 2 (n=3 patients) included all consecutive patients who spontaneously developed sustained organized tachycardias and received PF_{REV} applications to define the tachycardia circuits.

All patients underwent procedures under general anesthesia. A decapolar catheter was placed in the coronary sinus, an intracardiac echocardiography catheter (8F AcuNav; Siemens, Mountain View, CA) guided transseptal puncture, and the lattice-tip catheter was advanced into the LA through a steerable sheath (Agilis; Abbott, St. Paul, MN) via routine transfemoral venous access. Intravenous heparin was administered before

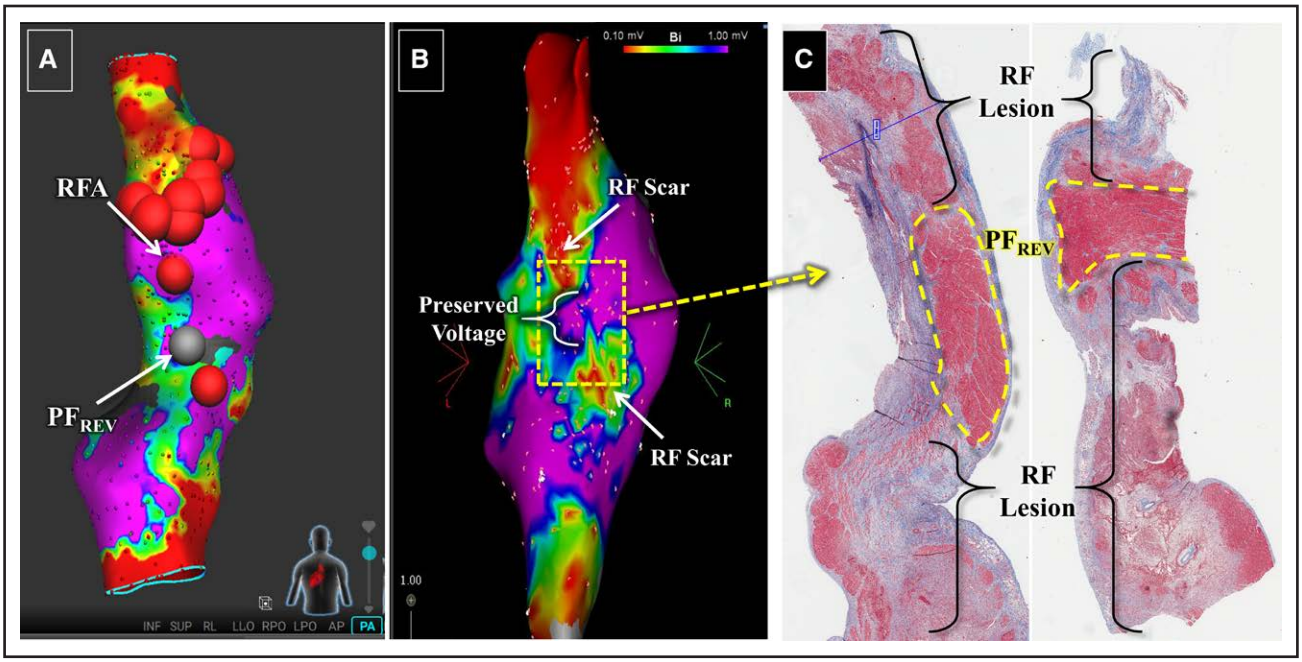

Figure 1. Effect of reversible pulsed electric field (PF_{REV}) on porcine atrial myocardium.
A, A single PF_{REV} application was placed between 2 discrete radiofrequency (RF) ablation lesions to facilitate identification of the PF_{REV} lesion in the chronic phase. **B**, The PF_{REV} lesion was identified as preserved voltage area in between RF scar on 3D voltage map. **C**, Histology demonstrated normal myocardium with no evidence of lesion formation between the 2 RF lesions.

transseptal puncture, with a goal activation clotting time between 300 and 350 s. The LA anatomy was rendered, followed by pulmonary vein isolation performed using either (1) PFA posteriorly and RFA anteriorly in the LA or (2) PFA both posteriorly and anteriorly.[14] Additional linear lesions included LA roof lines using PFA, mitral isthmus lines using PFA or RFA, and cavotricuspid isthmus lines using RFA. All clinical applications were of the low-dose pulse formulation ($PF_{REV-LOW}$).

Cohort Number 1

PF_{REV} energy was applied to the posterior LA at select discrete sites along the anticipated path or enclosed within a planned lesion set (eg, circumferential lesion set around PVs or center of posterior wall when a box lesion set is planned), including a single lesion at the anatomic slow pathway in 1 patient. After delivery of the PF_{REV} pulse, the catheter was maintained in position for ≈4 minutes while electrograms were continuously recorded. The amplitudes of bipolar electrograms were measured as described in preclinical experiment 1 above. In a few select cases, detailed high-density bipolar voltage electroanatomical maps were created at baseline, immediately after the PF_{REV} application, and at 1 minute post-PF_{REV}.

Cohort Number 2

Upon spontaneous development of an organized tachycardia, the electrophysiological mechanism was elucidated by standard activation and entrainment mapping maneuvers, including electroanatomical mapping of macro-reentrant tachycardia circuits. At putative critical sites, PFM was performed using a reversible microsecond-duration pulse train, as described above.[22,23] If a site demonstrated repeated termination by the PF_{REV} applications without local myocardial capture, ablative lesions (RFA or PFA) were administered at those sites to eliminate the target tachycardia.

Statistical Analysis

Continuous variables are expressed as mean±SD or median with interquartile range, and categorical variables are noted as count and percentage. Statistical analyses were performed with SPSS 24.0 software (SPSS, Inc, Chicago, IL).

RESULTS

Assessment of Reversibility: Atrial Myocardium

Preclinical: Experiment 1

In 6 animals, 8 PF_{REV} applications were placed at discrete sites along the RA septum (n=4), posterior RA (n=2), LA appendage (n=1), and RA appendage (n=1). The selected electrogram amplitude at baseline was 1.4±0.8 mV (range, 0.6–1.5 mV) and diminished to 0.3±0.2 mV after the PF_{REV} application, translating to a mean reduction of 74% (range, 51.2%–86.3%). This was accompanied by a loss of high-frequency components. As shown in Figure 3, there was a gradual recovery of the amplitude over the observation period. For the 4 electrograms that were followed out to 5 minutes, the amplitude recovered to 77.7% of baseline (range, 51.2%–86.3%). Pacing thresholds (assessed for 4 of 8 sites) increased from <1.0 mA at baseline to >10.0 mA immediately after the pulse; these subsequently recovered to 2.3±1.8 mA after 166±95 s.

These animals were survived for a mean of 12.2±1.3 days. Electroanatomic mapping at this time did not reveal any regions of low bipolar voltage (<0.1 mv) at the PF_{REV} delivery locations. At necropsy, there were no lesions at any of these locations.

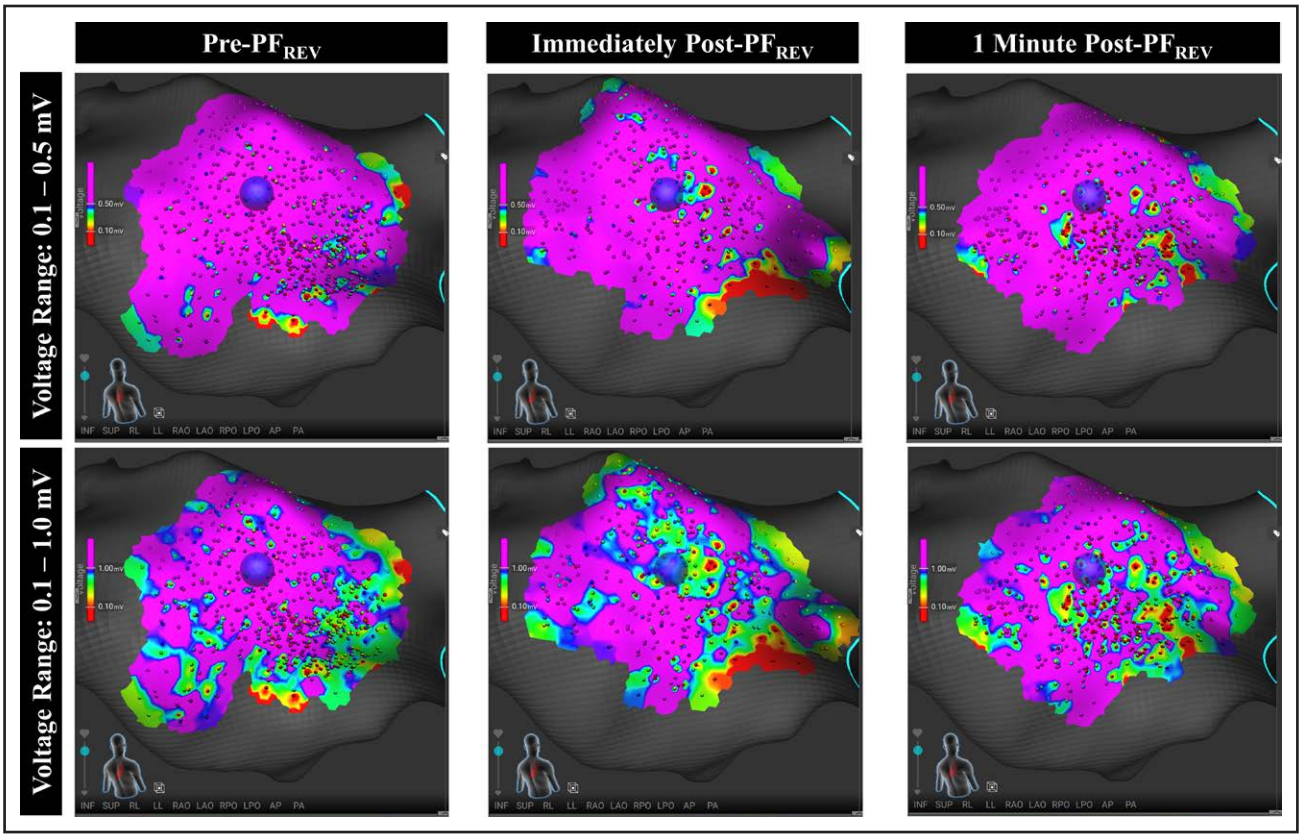

Figure 2. Effect of reversible pulsed electric field (PF$_{REV}$) on human atrial myocardium.
Detailed high-density electroanatomic maps were created at baseline, immediately after, and at 1 minute post-PF$_{REV}$ to display local bipolar voltage change. **Top** uses the bipolar voltage range of 0.10 to 0.50 mV, and **bottom** uses the bipolar voltage range of 0.10 to 1.00 mV.

In Figure 2, a single PF$_{REV}$ application was placed between 2 RFA lesions; at necropsy, a region of grossly spared myocardium between 2 obvious thermal lesions was observed. Three histological sections taken along its length revealed normal myocardium with no evidence of lesion formation. For other application sites where there was no grossly visible pathological evidence of lesion formation at the PF$_{REV}$ sites, histological evaluation was deferred.

Preclinical: Experiment 2

PF$_{REV}$ applications were successfully delivered within the appendages. After completing the 30-day survival period, on necropsy, there were no appreciable endocardial lesions visible in any of the 6 animals. Histological sectioning revealed scattered, shallow areas of superficial fibrosis observed along the endocardial aspect (Figure S2). The mean depth measured using histomorphometry was 0.5 mm (median, 0.4 [range, 0.1–1.3] mm).

Clinical: Cohort Number 1

In 9 patients, before any atrial ablation, a total of 14 PF$_{REV}$ applications were delivered at the following sites: right posterior PV antrum (n=5), left posterior PV antrum (n=3), anterior right PV antrum (n=3), mid-posterior LA wall (n=2), and slow pathway region (n=1). The mean electrogram amplitude at baseline was 4.2±2.5 mV (range, 0.55–8.13 mV) and demonstrated a maximum reduction of 69.9% (range, 34.5%–89.4%) immediately after PF$_{REV}$ delivery. Similar to the preclinical observations in experiment 1, there was gradual recovery of the electrogram to 84% of baseline (range, 56.7%–97.8%) by 3 minutes (Figure 3; Video S1). Detailed electroanatomical voltage mapping depicts the regional effect of a single PF$_{REV}$ application on the atrial myocardium (Figure 2). To limit the interruption of the AF ablation procedure, the observation period was not extended beyond 3 minutes to allow greater electrogram recovery.

Assessment of Reversibility: Porcine AV Node

Preclinical: Experiment 3

A total of 17 low-dose (PF$_{REV-LOW}$) and 10 high-dose (PF$_{REV-HIGH}$) pulses were delivered in 5 animals. In the PF$_{REV-LOW}$ group, there was no effect on AV conduction in 6 of 17 applications, transient PR prolongation (median, 40 [interquartile range, 10–136] ms) in 10 of 17 applications, and transient AV block in 1 of 17 applications (Table 1; Figure 4). Of these 11 applications with PR changes, there was 100% recovery of the PR interval to baseline in 9 of 11 applications within just 9.5 (interquartile range, 5–35) s. For the remaining 2 (of 11) applications, the PR recovered to within 10 and 30 ms of

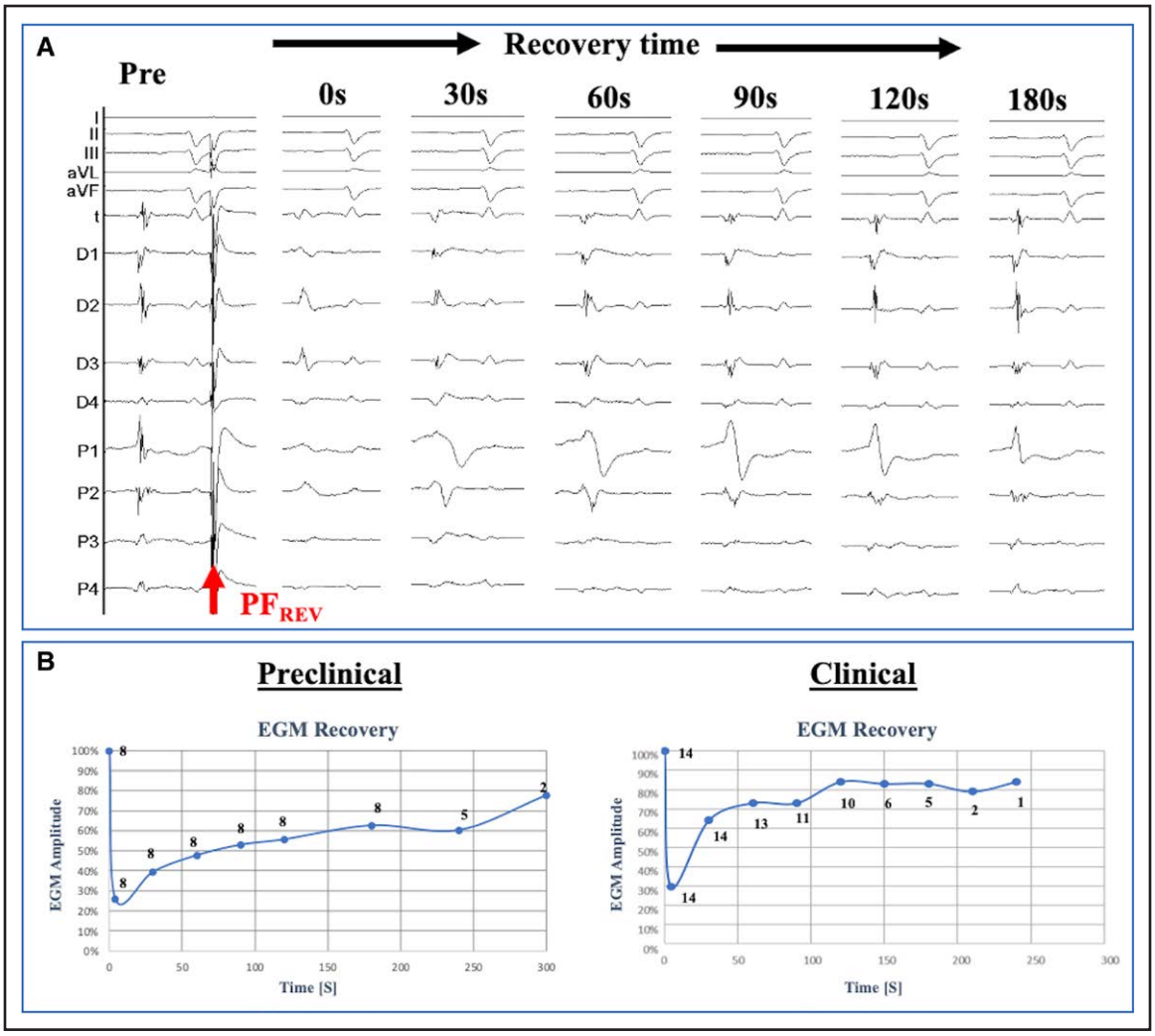

Figure 3. Atrial electrogram amplitude changes after reversible pulsed electric field (PF_{REV}).
A, Shown is an example of the acutely diminished electrograms observed on the mini-electrodes of the lattice catheter immediately after a PF_{REV} application (red arrow). Note the immediately diminished amplitude of the electrogram, with gradual recovery over time. **B**, Shown are the aggregate electrogram amplitude diminution data observed immediately after PF_{REV} in either porcine (n=6 animals, n=8 PF_{REV} applications; **left**) or human (n=9 patients, n=14 PF_{REV} applications; **right**) atrial myocardium. Note the acute decrease in the electrogram amplitude in both cohorts, followed by gradual recovery. The numbers indicate the total number of electrograms analyzed.

baseline by 60 s of observation. Complete recovery to baseline was not documented as the observation time was limited to 60 s.

In the $PF_{REV\text{-}HIGH}$ group, AV conduction changes occurred in 8 of 10 applications, of which PR prolongation alone and transient AV block occurred with 3 and 5 applications, respectively. There was complete recovery of the PR interval to baseline in all 8 (100%) within 105 s (interquartile range, 33–195).

Of note, for both groups, the His bundle potential was recorded in 15 of 27 (56%) applications (12/17 $PF_{REV\text{-}LOW}$ and 3/10 $PF_{REV\text{-}HIGH}$). For these 15 applications, the PR prolongation was identified to be confined to lengthening of the AH interval, that is, the HV interval remained constant in all instances. On the 4 recorded surface EKG leads, there were discernable QRS changes in 7 of 27 applications, all of which resolved during the observation period.

Assessment of Reversibility: In Vivo Tachycardia Circuits

Patient Details

Details of the 3 cohort number 2 patients are shown in Table 2: all had a history of persistent AF resistant to class I or III antiarrhythmic drugs, preserved left ventricular systolic function, and LA diameters between 45 and 50 mm. During ablation, PVI and linear atrial lesions were successfully placed without electrical conduction breakthrough (including at the LA roof, cavotricuspid isthmus, and, in 2 of 3 patients, the posterior mitral isthmus; Table 2).

Patient Number 1

Following ablation of typical RA flutter at the cavotricuspid isthmus, there was spontaneous atypical atrial flutter with a variable rate: cycle lengths of 340 or

Table 1. Effect of PF_{REV} Energy on the Porcine AV Node

	$PF_{REV-LOW}$ (n=17)	$PF_{REV-HIGH}$ (n=10)
No effect	6/17 (35%)	2/10 (20%)
AV prolongation, ms	40 (IQR, 10–136; n=10)	64 (IQR, 15–NA; n=3)
Transient AV block	1/17 (6%)	5/10 (50%)
Time to AV conduction recovery, s	9.5 (IQR, 5–35; n=9)	105 (IQR, 33–195; n=8)

AV indicates atrioventricular; IQR, interquartile range; NA, not available; and PF_{REV}, reversible pulsed electric field.

380 ms, translating to atrial rates of 158 to 176 bpm. Entrainment from the low lateral RA resulted in a long postpacing interval (Figure S3), thereby implicating the LA. High-density LA activation mapping revealed 2 potential mechanisms for the tachycardia: either focal or a macro-reentry (Figure 5A; Video S2). Definitively discriminating between these diagnoses was challenged by the combination of (1) marked electrogram fractionation along the atrial septum, which precluded accurate timing annotation (Figure 5A, inset), and (2) the variable flutter cycle length, complicating entrainment maneuvers.

Accordingly, the PF_{REV} applications were placed along the atrial septum, causing termination of the 340- and 380-ms flutters closer and further from the mitral annulus, respectively (Figure 5B; Figure S4). A series of RFA lesions at this region terminated (Video S3) and rendered the flutters noninducible. Then, the AF ablation lesion set was placed, followed by additional anterior LA lesions to this region extended to the right pulmonary veins (Figure S5; Video S4).

Patient Number 2

After PVI and roofline ablation, AF organized to an atypical flutter (cycle length, 215 ms). Activation mapping revealed a figure-of-8 reentry pattern: one limb being localized to the LA anterior wall and the other limb, a perimitral circuit (Figure S6; Video S5). A PF_{REV} application at the convergence of the 2 limbs of the circuit, along the anterior atrium near the mitral annulus, terminated the flutter; subsequently, 4 PFA lesions rendered this rhythm noninducible. Finally, a mitral isthmus line was placed, and after the induction of typical RA flutter, a cavotricuspid isthmus line terminated this flutter (Figure S7).

Patient Number 3

After PVI and linear lesions, a narrow-complex tachycardia (cycle length, 500 ms) with 1:1 atrial-to-ventricular response occurred spontaneously and was easily inducible (Figure 6A). Atrioventricular nodal tachycardia (AVNRT) was diagnosed by standard electrophysiological maneuvers: facile reinduction dependent on an AH jump, V-A-V response with ventricular entrainment, short His-atrial electrogram timing, and para-Hisian pacing consistent with atrioventricular nodal conduction only.

When a series of PF_{REV} pulses were delivered to the RA septum, AVNRT terminated and was not immediately reinducible at one specific location consistent with a slow pathway site (Figure 6B and 6C; Video S6); the rhythm was unaffected by PF_{REV} applications at adjacent noncritical sites (Figure 6B and 6D; Video S7). Immediately after termination, an AH jump was not elicited and AVNRT was not reinducible, but 1 to 2 minutes later, both the jump and reinducibility were observed. A single

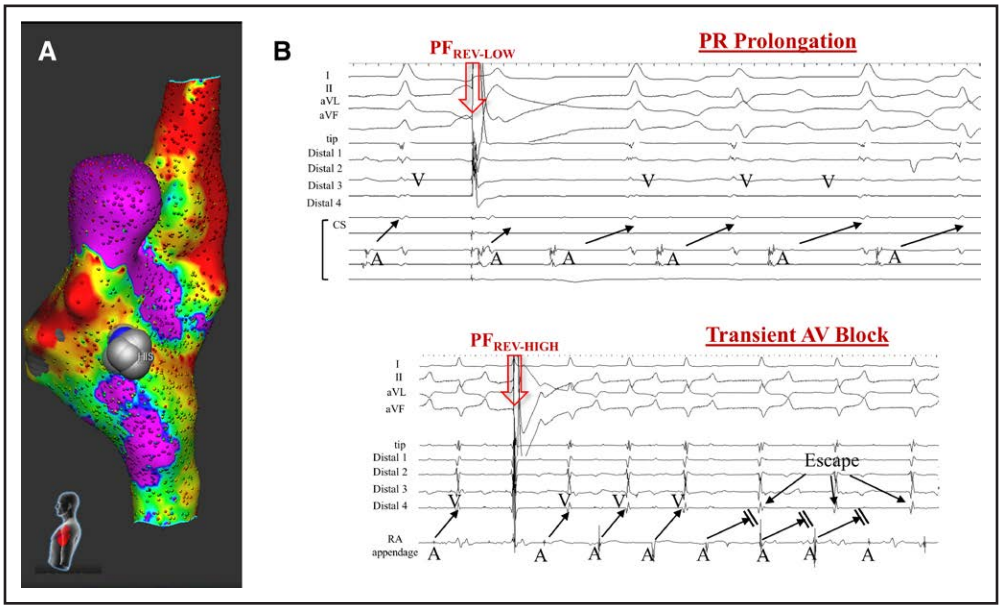

Figure 4. Effect of reversible pulsed electric field (PF_{REV}) on the porcine AV node.
A, $PF_{REV-LOW}$ and $PF_{REV-HIGH}$ were placed at the site of the His potential. **B**, PR prolongation was predominantly observed with $PF_{REV-LOW}$, whereas temporal AV block was frequently introduced in $PF_{REV-HIGH}$.

Table 2. Tachycardia Patients: Clinical and Procedural Characteristics

	Case Number 1	Case Number 2	Case Number 3
Age, y	70	59	50
Gender	Male	Male	Male
Body mass index, kg/m^2	28.7	26.8	32.7
Medical history			
Type of AF	Persistent AF	Persistent AF	Persistent AF
CHA_2DS_2-VASc score	2	1	1
Hypertension, Y/N	Y	N	Y
Diabetes, Y/N	N	Y	N
LVEF, %	45	65	60
LA dimension, mm	45	46	48
Oral anticoagulant	Apixaban	Apixaban	Edoxaban
Antiarrhythmic drugs	Amiodarone	Propafenone	Amiodarone
Ablation lesions, energy employed			
Pulmonary vein isolation	RF/PF	PF	RF/PF
LA roof line	PF	PF	PF
Mitral isthmus line	…	PF	RF
Cavotricuspid isthmus Line	RF	PF	RF
Organized tachycardia			
Mechanism	Atypical LA flutter	Atypical LA flutter	AVNRT
Cycle length, ms	340–380	230	500
Atrial rate, bpm	158–176	279	120
Ablation energy Employed	RF	PF	RF
No. of ablation lesions	8	4	1
Ablation energy Duration, sec	40	16.1	3
Fluoroscopy time, min	6.6	0	11.7
Saline infused, mL	1045	521	869
Complications	None	None	None
Follow-up			
Duration of follow-up, mo*	12	12	12
Tachycardia Recurrences?	None	None	None

AF indicates atrial fibrillation; AVNRT, atrioventricular nodal tachycardia; bpm, beats per minute; LA, left atrium; LVEF, left ventricular ejection fraction; N, no; PF, pulsed field; RF, radiofrequency; and Y, yes.

*As per protocol, maximum duration of follow-up is 12 mo.

radiofrequency lesion at this location terminated the AVNRT, rendering it noninducible (Figure S8; Video S8).

DISCUSSION

In this proof-of-principle analyses of PF_{REV}, using a combination of preclinical and clinical studies, we demonstrated the following observations: (1) when delivered to porcine atrial tissue, PF_{REV} energy acutely diminished the bipolar electrogram by 74%, with subsequent gradual recovery to 78% of baseline by 5 minutes; (2) similarly, for LA PF_{REV} applications delivered to patients with AF, the electrograms diminished by 70%, with subsequent recovery to 84% by 3 minutes; (3) pathological analyses revealed either no evidence of lesions at the sites targeted or only superficial focal fibrosis; and (4) when delivered to the AV node, PF_{REV} energy caused dose-dependent transient changes in AV nodal conduction that fully recovered. Together, these observations supported the delivery of partially reversible pulses to putative critical regions of stable tachycardia circuits to adjudicate their suitability as potential targets, before delivering tissue-destructive ablation lesions. And indeed, the proof of principle of this conceptualized novel strategy of PFM was established by terminating tachycardias with PF_{REV} applications to potentially important sites, thereby establishing their criticality to the circuits before subsequent successful ablation.

Reversible Effects of Pulsed Electric Fields

During PFA, tissue destruction is a consequence of the ablative electric field that is created around the catheter electrodes. Lesions are created when the field exceeds a certain threshold determined by various factors including the tissue type and pulse parameters such as voltage, duration, repetition, etc.[2] On the other hand, abbreviated reversible pulses create sublethal fields that transiently increase cell membranes permeability without subsequent cell death. Indeed, reversible electroporation has been successfully used in cell biology to introduce exogenous material such as DNA into cells.[20,21]

Because of the unique conductive properties of myocardial tissue, transient cell membrane changes readily manifest as electrical changes. Such effects have been long recognized, for example, transient ST-segment elevation after defibrillation, and more recently, transient ST-segment elevation after monophasic PFA of LA tissue.[8] Other instances of more localized myocardial changes have also been described. In an open-chest, canine study of epicardial atrial activation, defibrillation pulses of varying intensity resulted in voltage-dependent temporary conduction block.[24] Other transient changes, such as a reduction in action potential amplitude and rate of rise of the action potential upstroke, have also been described.[22,23,25–27] The availability of modern PF generators and focal catheters allowed us to investigate the effects of such reversible pulses applied to myocardial tissue.

Electrophysiological Effects of Reversible Pulses

Both the preclinical and clinical assessments demonstrated an immediate and significant (60%–80%)

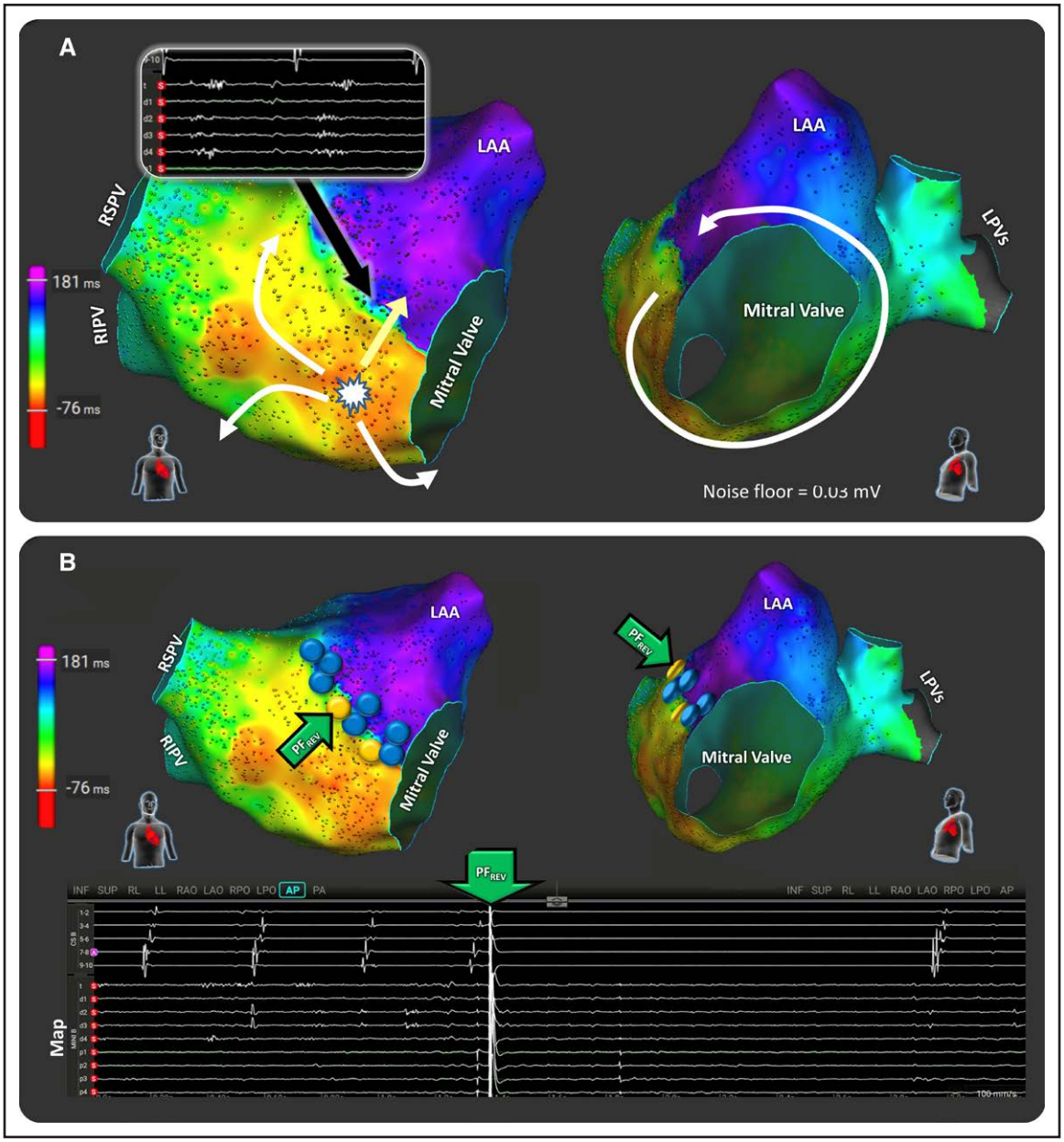

Figure 5. Atypical atrial flutter: potential mechanisms and the effect of reversible PF pulses.
A, When the left atrium was mapped during the spontaneous atypical atrial flutter in patient number 1, the activation pattern was consistent with 2 potential mechanisms: (1) a focal tachycardia with a site of origin in the low anterior left atrium near the mitral valve (**left**) or (2) a macro-reentrant flutter circumventing around the mitral annulus (**right**). In these activation maps, the color bar indicates the order of activation with the earliest being in red and the latest in purple (see Video S2 for a propagation map that more clearly depicts these potential mechanisms). Note in the inset the highly fractionated, long-duration electrograms observed on the catheter mini-electrodes, which contribute to the confusion on the mechanism since they complicate proper annotation of local timing. The left atrial shell is shown in the anteroposterior (**left**) and left anterior oblique caudal (**right**) views. **B**, A reversible pulsed electric field (PF_{REV}) application at the yellow tag terminated the ongoing rhythm. The views of the left atrium are the same as in **A**. CS, coronary sinus; LAA, left atrial appendage; LPVs, left pulmonary veins; Map, mapping catheter; RIPV, right inferior pulmonary vein; RSPV, right superior pulmonary vein.

reduction in atrial electrogram amplitude with PF_{REV} applications. This was followed by ≈80% recovery of the bipolar voltage amplitude by the 3- to 5-minute timepoint. The amplitude changes were mirrored by changes in pacing threshold assessment: an acute rise with no capture (at 10 mA at 2 ms) followed by significant improvement in the thresholds over time. Given that PF_{REV} delivery was limited to focal applications, we were unable to ascertain conduction block (except in the below AV nodal assessments), as well as the time course of changes in conduction velocities.

On the other hand, when the PF_{REV} applications were administered to AV nodal tissue, dose-dependent conduction changes were observed immediately after the

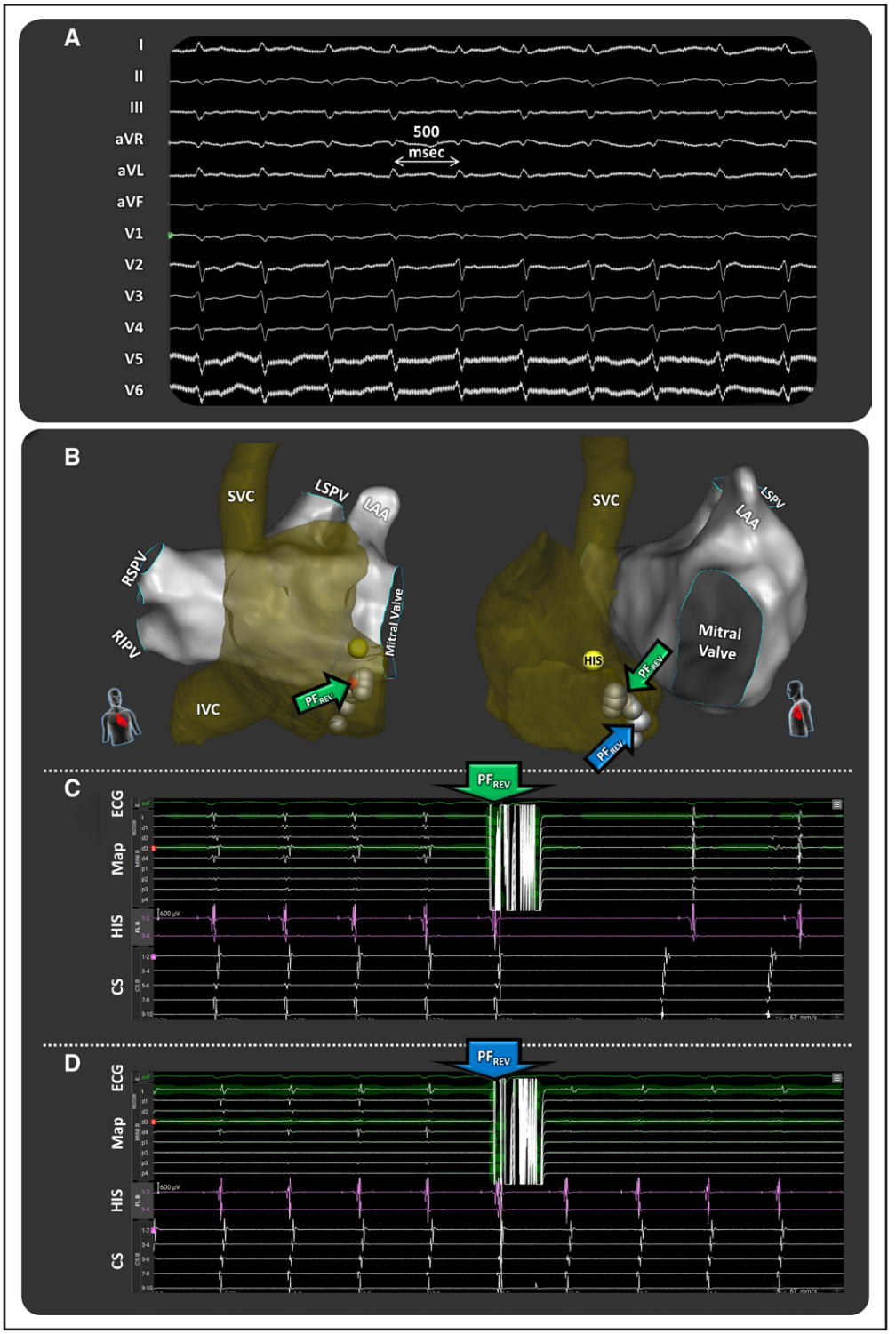

Figure 6. Identification of the slow pathway region to guide ablation of atrioventricular nodal tachycardia.
A, In patient number 3, after the atrial fibrillation ablation lesion set, this supraventricular tachycardia (500 ms=120 bpm) occurred spontaneously and was demonstrated to be atrioventricular nodal reentrant tachycardia by standard electrophysiological maneuvers. **B**, A limited right atrial geometry is shown (transparent yellow) adjacent to the left atrial anatomy (silver) in either right anterior oblique (**left**) or steep left anterior oblique (**right**) views. The silver and red tags represent locations where reversible pulsed electric field (PF_{REV}) applications were delivered. This resulted in either (1) termination of the tachycardia, consistent with the site being critical for the tachycardia (red tag; **C**; Video S6) or (2) no effect on the tachycardia (silver tags; **D**; Video S7), consistent with not being critical for the tachycardia circuit. CS indicates coronary sinus; HIS, His bundle catheter; LAA, left atrial appendage; LIPV, left inferior pulmonary vein; LSPV, left superior pulmonary vein; Map, mapping catheter; RIPV, right inferior pulmonary vein; and RSPV, right superior pulmonary vein.

pulse. Conduction changes (PR prolongation or transient AV block) occurred more frequently with the higher dose reversible pulse. Similarly, transient heart block was also more common with the higher dose reversible pulses (5/10 versus 1/17). The time course of recovery was also more gradual with the higher dose PF_{REV} applications (≈100 versus 10 s), consistent with dose-related response.

For electrogram amplitude diminution assessment, ≈80% recovery of amplitude was observed by the 5-minute timepoint. It should be noted that recordings beyond these timepoints were not performed for practical reasons (limiting the duration of the experiments). It is indeed possible that complete or near-complete electrogram amplitude recovery might have occurred if monitoring had been extended. As for the AV nodal assessment, it must be emphasized that multiple applications were applied at the same location in some animals (ie, PF_{REV} application, followed by significant recovery, followed by additional PF_{REV} application). Accordingly, potential cumulative effects of repeated applications may have played a role in the degree and speed of observed conduction recovery.

Pathological Analysis of Reversible Pulses

Histological assessment of tissues exposed to PF_{REV} pulses revealed almost complete sparing of the myocardium. Only scattered, superficial (≈0.5 mm depth) areas of fibrosis were noted in the RA appendage, whereas no changes were noted in the RA. It is possible that PF_{REV} effects were exaggerated in the appendage, where the 9-mm lattice tip catheter was in intimate contact with surrounding trabeculae, potentially resulting in exaggerated tissue effects and thus accounting for the observed (albeit superficial) lesions.

Indeed, it is likely that further evolution in the PF_{REV} waveform characteristics might result in a pulse with even less superficial myocardial changes. On the other hand, even if mild, submillimeter depth fibrosis is unavoidable, given the minimal impact it would have on local myocardial function, one could still use PF_{REV} energy to electrically interrogate atrial tissue to assess its relevance when applied judiciously. After all, if the PF_{REV} energy was not used, it is not uncommon in clinical practice to simply apply a test lesion to see whether ablative energy has an impact. Indeed, the minimal amount of damage becomes less relevant if the site of application is either within the path of the putative target site for ablation or in the vicinity of scarred myocardium.

A good predicate to PFM is cryomapping, which was introduced in the late 1990s: this technique of cooling tissue to sublethal temperatures can also reversibly affect local myocardial electrical properties.[28,29] Just like with PF_{REV}, cryomapping was also associated with surface fibrosis in preclinical studies. Accordingly, cryomapping has been used safely over the past 2 decades. On the other hand, cryomapping is slow, requires a specialized focal cryocatheter that is infrequently used in clinical practice, and thus has not made any meaningful impact on clinical practice. In contrast, PF_{REV} applications could certainly be delivered from any catheter with electrodes, amplifying the applicability of PFM.

Tachycardia Case Series

The present case series demonstrates the feasibility of identifying ablation-sensitive critical sites for the target tachycardias in a workflow-conducive manner. The specificity of these sites was highlighted by both (1) the absence of effect of reversible pulses when applied to adjacent sites noncritical for tachycardia maintenance (Figure 6D; Figure S4B) and (2) the termination and noninducibility of the respective tachycardias by ablation at the critical sites. Furthermore, the first case was complex because of both the variability in tachycardia rate and the duration of the fractionated electrogram; in this case, the reversible pulses were instrumental in elucidating not only an ideal site of ablation but also that the mechanism of the tachycardia was macro-reentry instead of focal.

Two aspects of the AVNRT case were interesting. First, after the reversible pulse terminated the arrhythmia, the lingering effect on the slow pathway prevented reinducibility for a few minutes, corroborating the physiology of the arrhythmia. Second, the tachycardia was eliminated with a single radiofrequency lesion, striking since AVNRT ablation using conventional thermal energy (radiofrequency or cryoablation) typically requires multiple lesions at multiple locations. While the large footprint of the lattice tip undoubtedly contributed to efficiency, the ability to adjudicate putative target sites with PF_{REV} applications was likely instrumental; this should be confirmed in large studies.

Limitations

This report is limited to the assessment of PF_{REV} applied to atrial and AV nodal tissue in healthy porcine myocardium and in patients undergoing AF ablation; indeed it should be considered exploratory and not a final dosing strategy that can be used for all clinical arrhythmias. Given the minimal endocardial PF footprint of these doses, the lack of demonstration of complete reversibility in electrogram amplitudes and pacing thresholds, and the small sample size of these experiments, this approach should not be assumed to be a completely reversible dose. We, therefore, recommend limiting its use to areas of scarred atrial tissue with regions thought to be critical tachycardia isthmus sites that are otherwise being considered for placing ablation lesions. Thus, while it is reasonable to surmise that PFM could also be applied to interrogate the physiology of other

atrial sites critical to supraventricular tachycardia circuits, this needs to be explored in future studies. The limited post-PF_{REV} observation periods (<5 minutes) preclude an understanding of the time duration needed for 100% recovery of electrogram amplitude and pacing thresholds. Accordingly, we emphasize that this report is unable to accurately describe the spatial effects of reversible PFA, both in terms of the endocardial dimension and depth. Additional detailed dosing studies are needed to determine the parameters that demarcate reversible from irreversible lesions, and its use in healthy myocardium at this time should be avoided.

Comprehensive electrophysiological assessment of parameters such as refractory periods and conduction velocities was not performed. The occurrence of histopathological changes with PF_{REV}, noted to be none to minimal in this report, would benefit from a larger histological study. Furthermore, careful dosing experiments are required to evaluate both PF_{REV} of various magnitude and of variable distance of the pulses to the target location. Additional studies are necessary for (1) corroboration in a larger cohort of patients, (2) expansion to other arrhythmia physiologies such as atrioventricular bypass tracts, (3) defining the depth and duration of effect, and (4) determining whether such pulses can also facilitate mapping of focal arrhythmias.

Conclusions

Together, these observations demonstrate the proof of principle that pulsed electrical fields can be delivered in vivo in a partially reversible manner such that by virtue of their transitory effect on cellular excitability, the physiology of tachycardia circuits can be elucidated. This novel concept of PFM could have far-reaching implications in the field of cardiac electrophysiology.

ARTICLE INFORMATION

Received January 23, 2023; accepted August 29, 2023.

Affiliations

Helmsley Electrophysiology Center, Icahn School of Medicine at Mount Sinai, New York, NY (J.S.K., I.K., K.K., V.Y.R.). Department of Cardiology, Homolka Hospital, Prague, Czech Republic (P.N., J.P., M.F., A.A., V.Y.R.). Department of Cardiovascular Diseases, Vilnius University, Lithuania (G.R.).

Sources of Funding

These cases were performed as part of a study funded by Affera, Inc.

Disclosures

Dr Reddy: Affera-Medtronic: consultant, equity (stock); other disclosures not related to this article are detailed in the Supplemental Material. Dr Koruth: Affera-Medtronic: grant support, stock, consultant. Dr Neuzil: Affera-Medtronic: grant support.

Supplemental Material

Supplemental Methods
Additional Disclosures
Figures S1–S8
Videos S1–S8

REFERENCES

1. Patel AM, d'Avila A, Neuzil P, Kim SJ, Mela T, Singh JP, Ruskin JN, Reddy VY. Atrial tachycardia after ablation of persistent atrial fibrillation: identification of the critical isthmus with a combination of multielectrode activation mapping and targeted entrainment mapping. *Circ Arrhythmia Electrophysiol.* 2008;1:14–22. doi: 10.1161/CIRCEP.107.748160
2. Batista Napotnik T, Polajžer T, Miklavčič D. Cell death due to electroporation - a review. *Bioelectrochemistry.* 2021;141:107871. doi: 10.1016/j.bioelechem.2021.107871
3. van Driel VJ, Neven K, van Wessel H, Vink A, Doevendans PA, Wittkampf FH. Low vulnerability of the right phrenic nerve to electroporation ablation. *Heart Rhythm.* 2015;12:1838–1844. doi: 10.1016/j.hrthm.2015.05.012
4. Neven K, van Es R, van Driel V, van Wessel H, Fidder H, Vink A, Doevendans P, Wittkampf F. Acute and long-term effects of full-power electroporation ablation directly on the porcine esophagus. *Circ Arrhythm Electrophysiol.* 2017;10:e004672. doi: 10.1161/CIRCEP.116.004672
5. Koruth J, Kuroki K, Iwasawa J, Enomoto Y, Viswanathan R, Brose R, Buck ED, Speltz M, Dukkipati SR, Reddy VY. Preclinical evaluation of pulsed field ablation: electrophysiological and histological assessment of thoracic vein isolation. *Circ Arrhythm Electrophysiol.* 2019;12:e007781. doi: 10.1161/CIRCEP.119.007781
6. Stewart MT, Haines DE, Verma A, Kirchhof N, Barka N, Grassl E, Howard B. Intracardiac pulsed field ablation: proof of feasibility in a chronic porcine model. *Heart Rhythm.* 2019;16:754–764. doi: 10.1016/j.hrthm.2018.10.030
7. Koruth JS, Kuroki K, Kawamura I, Brose R, Viswanathan R, Buck ED, Donskoy E, Neuzil P, Dukkipati SR, Reddy VY. Pulsed field ablation vs radiofrequency ablation: esophageal injury in a novel porcine model. *Circ Arrhythm Electrophysiol.* 2020;13:e008303. doi: 10.1161/CIRCEP.119.008303
8. Koruth JS, Kuroki K, Kawamura I, Stoffregen WC, Dukkipati SR, Neuzil P, Reddy VY. Focal pulsed field ablation for pulmonary vein isolation and linear atrial lesions: a preclinical assessment of safety and durability. *Circ Arrhythm Electrophysiol.* 2020;13:e008716. doi: 10.1161/CIRCEP.120.008716
9. Cochet H, Nakatani Y, Sridi-Cheniti S, Cheniti G, Ramirez FD, Nakashima T, Eggert C, Schneider C, Viswanathan R, Derval N, et al. Pulsed field ablation selectively spares the oesophagus during pulmonary vein isolation for atrial fibrillation. *Europace.* 2021;23:1391–1399. doi: 10.1093/europace/euab090
10. Reddy VY, Koruth J, Jais P, Petru J, Timko F, Skalsky I, Hebeler R, Labrousse L, Barandon L, Kralovec S, et al. Ablation of atrial fibrillation with pulsed electric fields: an ultra-rapid, tissue-selective modality for cardiac ablation. *JACC Clin Electrophysiol.* 2018;4:987–995. doi: 10.1016/j.jacep.2018.04.005
11. Reddy VY, Neuzil P, Koruth JS, Petru J, Funosako M, Cochet H, Sediva L, Chovanec M, Dukkipati SR, Jais P. Pulsed field ablation for pulmonary vein isolation in atrial fibrillation. *J Am Coll Cardiol.* 2019;74:315–326. doi: 10.1016/j.jacc.2019.04.021
12. Loh P, van Es R, Groen MHA, Neven K, Kassenberg W, Wittkampf FHM, Loh P, Doevendans PA. Pulmonary vein isolation with single pulse irreversible electroporation: a first in human study in 10 patients with atrial fibrillation. *Circ Arrhythm Electrophysiol.* 2020;13:e008192. doi: 10.1161/CIRCEP.119.008192
13. Reddy VY, Anic A, Koruth J, Petru J, Funasako M, Minami K, Breskovic T, Sikiric I, Dukkipati SR, Kawamura I, et al. Pulsed field ablation in patients with persistent atrial fibrillation. *J Am Coll Cardiol.* 2020;76:1068–1080. doi: 10.1016/j.jacc.2020.07.007
14. Reddy VY, Anter E, Rackauskas G, Peichl P, Koruth JS, Petru J, Funasako M, Minami K, Natale A, Jais P, et al. Lattice-tip focal ablation catheter that toggles between radiofrequency and pulsed field energy to treat atrial fibrillation: a first-in-human trial. *Circ Arrhythm Electrophysiol.* 2020;13:e008718. doi: 10.1161/CIRCEP.120.008718
15. Reddy VY, Dukkipati SR, Neuzil P, Anic A, Petru J, Funasako M, Cochet H, Minami K, Breskovic T, Sikiric I, et al. Pulsed field ablation of paroxysmal atrial fibrillation: one-year outcomes of IMPULSE, PEFCAT & PEFCAT II. *JACC Clin Electrophysiol.* 2021;7:614–627. doi: 10.1016/j.jacep.2021.02.014
16. Verma A, Boersma L, Haines DE, Natale A, Marchlinski FE, Sanders P, Calkins H, Packer DL, Hummel J, Onal B, et al. First-in-human experience and acute procedural outcomes using a novel pulsed field ablation system: the PULSED AF pilot trial. *Circ Arrhythm Electrophysiol.* 2022;15:e010168. doi: 10.1161/CIRCEP.121.010168
17. Ekanem E, Reddy VY, Schmidt B, Reichlin T, Neven K, Metzner A, Hansen J, Blaauw Y, Maury P, Arentz T, et al; MANIFEST-PF Cooperative. Multi-National Survey on the Methods, Efficacy and Safety on the

Post-Approval Clinical Use of Pulsed Field Ablation (MANIFEST-PF). *Europace*. 2022;24:1256–1266. doi: 10.1093/europace/euac050
18. Bolhassani A, Khavari A, Orafa Z. Electroporation – advantages and drawbacks for delivery of drug, gene and vaccine. In: Sezer AD eds. *Application of Nanotechnology in Drug Delivery*. 2014, InTech.
19. Kotnik T, Rems L, Tarek M, Miklavcic D. Membrane electroporation and electropermeabilization: mechanisms and models. *Annu Rev Biophys*. 2019;48:63–91. doi: 10.1146/annurev-biophys-052118-115451
20. Harrison RL, Byrne BJ, Tung L. Electroporation-mediated gene transfer in cardiac tissue. *FEBS Lett*. 1998;435:1–5. doi: 10.1016/s0014-5793(98)00987-9
21. Rosen MR, Brink PR, Cohen IS, Robinson RB. Genes, stem cells and biological pacemakers. *Cardiovasc Res*. 2004;64:12–23. doi: 10.1016/j.cardiores.2004.05.012
22. Neunlist M, Tung L. Dose-dependent reduction of cardiac transmembrane potential by high-intensity electrical shocks. *Am J Physiol*. 1997;273:H2817–H2825. doi: 10.1152/ajpheart.1997.273.6.H2817
23. Aguel F, DeBruin KA, Krassowska W, Trayanova NA. Effects of electroporation on the transmembrane potential distribution in a two-dimensional bidomain model of cardiac tissue. *J Cardiovasc Electrophysiol*. 1999;10:701–714. doi: 10.1111/j.1540-8167.1999.tb00247.x
24. Yabe S, Smith WM, Daubert JP, Wolf PD, Rollins DL, Ideker RE. Conduction disturbances caused by high current density electric fields. *Circ Res*. 1990;66:1190–1203. doi: 10.1161/01.res.66.5.1190
25. De Bruin KA, Krassowska W. Modeling electroporation in a single cell. II. Effects of ionic concentrations. *Biophys J*. 1999;77:1225–1233. doi: 10.1016/S0006-3495(99)76974-2
26. De Bruin KA, Krassowska W. Modeling electroporation in a single cell. I. Effects of field strength and rest potential. *Biophys J*. 1999;77:1213–1224. doi: 10.1016/S0006-3495(99)76973-0
27. Nikolski VP, Sambelashvili AT, Krinsky VI, Efimov IR. Effects of electroporation on optically recorded transmembrane potential responses to high-intensity electrical shocks. *Am J Physiol Heart Circ Physiol*. 2004;286:H412–H418. doi: 10.1152/ajpheart.00689.2003
28. Dubuc M, Roy D, Thibault B, Ducharme A, Tardif JC, Villemaire C, Leung TK, Talajic M. Transvenous catheter ice mapping and cryoablation of the atrioventricular node in dogs. *Pacing Clin Electrophysiol*. 1999;22:1488–1498. doi: 10.1111/j.1540-8159.1999.tb00353.x
29. Skanes AC, Dubuc M, Klein GJ, Thibault B, Krahn AD, Yee R, Roy D, Guerra P, Talajic M. Cryothermal ablation of the slow pathway for the elimination of atrioventricular nodal reentrant tachycardia. *Circulation*. 2000;102:2856–2860. doi: 10.1161/01.cir.102.23.2856